VIP Submicrometer Spheres

DOI: 10.1002/anie.201002963

Selective Pulsed Heating for the Synthesis of Semiconductor and Metal Submicrometer Spheres**

*Hongqiang Wang, Alexander Pyatenko, Kenji Kawaguchi, Xiangyou Li, Zaneta Swiatkowska-Warkocka, and Naoto Koshizaki**

Spherical particles are of great interest because they are a thermodynamically favorable state in terms of surface energy. Recent work has fully demonstrated their potential to obtain interesting and useful functionalities in many fields of application, such as photonic crystals, biomedicine, sensing, catalysis, environmental remedies, and solar cells.[1] Submicrometer spheres, with sizes ranging from 0.1 to 1 μm, are particularly useful in medical fields because of their unique size-related capability of selectively entering tumor cells. In particular, the synthesis of submicrometer spheres has recently become much more urgent owing to increasing concern about the evaluation of nanosize-dependent biotoxicity.[2] Numerous techniques have been devised in an effort to produce spheres of dielectric materials, such as polystyrene (PS), SiO_2, and poly(methyl methacrylate) (PMMA) in copious quantities and with suitable diameters.[3] However, it is surprising to note that until now, the synthesis of semiconductor and metal submicrometer spheres, which are expected to offer broad and promising advantages over dielectric materials owing to their distinctive electrical, optical, magnetic, thermoelectric, and optoelectric properties, has rarely been discussed in the literature.[4] The reason for this is that the crystal behavior of semiconductors and metals always causes them to grow anisotropically, with a high tendency to form non-spherical nanostructures. To date, most studies have been constrained to the synthesis of spherical secondary structures assembled by nanostructures.[1,5] Despite demonstrated novel functionalities, the lack of close contact between nanostructures will inevitably influence or even reduce the performance of submicrometer spheres in electric, magnetic, optoelectric, and thermoelectric applications. Seeking general strategies to create semiconductor and metal submicrometer spheres constructed without any subunits, especially those with smooth surfaces, which enable the uniform surface immobilization of bioactive molecules in biomedical fields, is thus highly desirable.

Conventional heating often relies on thermal conduction of black-body radiation to drive chemical reactions, in which thermal energy is transferred from the heating source to the solvent and finally to the reactant molecules. This provides continuous heating (both temporally and spatially) for semiconductor/metal nucleus formation and subsequent preferential crystal growth; it is thus kinetically difficult to inhibit anisotropic crystal growth. One effective method of overcoming this problem has been developed by Xia and coworkers by quenching pre-melted metal spheres to retain their spherical morphology.[4b] However, it is difficult to melt most semiconductors and metals using conventional heating because the reaction temperature is determined by the solvent, and solvents with high boiling points are currently very limited. Consequently, inhibiting anisotropic crystal growth and melting semiconductor/metal particles are critical requirements for synthesizing semiconductor/metal submicrometer spheres, which is currently bottlenecked by the heating mechanism of conventional heating.

Herein, we describe an innovative selective pulsed heating method involved in the pulsed laser irradiation of colloidal nanoparticles (PLICN), which is found to be encouragingly general for the synthesis of size-tailored semiconductor and metal submicrometer spheres with smooth surfaces. This new finding could be of great use for the extensive exploration of submicrometer-sphere-based research. Figure 1 illustrates the concept of selective pulsed heating, which is unique to address the aforementioned problems. As shown in Figure 1a, instantaneous heating can be completed within 10 ns (typical for an Nd:YAG laser with pulse width of 10 ns and repetition rate of 30 Hz), followed by a subsequent quenching process that usually takes 10^{-6} to 10^{-4} s.[6] Because the quenching time is much shorter than the interval between two consecutive pulses, the pulsed laser irradiation process is actually an

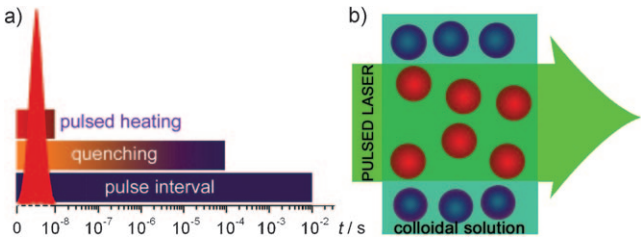

Figure 1. The selective pulsed heating involved in pulsed laser irradiation of colloidal nanoparticles. a) Temporal discontinuity: pulsed heating and subsequent quenching, and b) spatial discontinuity: only the particles are heated, not the solvent.

[*] Dr. H. Wang, Dr. A. Pyatenko, Dr. K. Kawaguchi, Dr. X. Li, Dr. Z. Swiatkowska-Warkocka, Prof. N. Koshizaki
Nanosystem Research Institute, National Institute of Advanced Industrial Science and Technology (AIST)
Tsukuba Central 5, 1-1-1 Higashi, Tsukuba, Ibaraki 305-8565 (Japan)
Fax: (+81) 29-861-6355
E-mail: koshizaki.naoto@aist.go.jp

[**] This work was partially supported by Grants-in-Aid for Scientific Research (B) (20360340).

Supporting information for this article is available on the WWW under http://dx.doi.org/10.1002/anie.201002963.

accumulation of numerous individual heating pulses. This temporally discontinuous heating could greatly inhibit the anisotropic growth of particles, thus allowing for the formation of particles with spherical geometry. Pulsed heating is also spatially discontinuous (see Figure 1b). When a pulsed laser is applied to the colloidal solution, only the nanoparticles are heated, not the solvent. This selective heating relies on the laser energy absorption of solid particles as well as the lack of thermal energy transfer to the solvent. If sufficient laser energy is absorbed, the particles will melt or even evaporate, even in low-boiling-point solvents.[6]

Figure 2a illustrates the morphology of the raw CuO nanoparticles. The sizes of most particles are below 50 nm, whilst a few are more than 100 nm. The particle size distribution histogram (Figure 2b) indicates that the average

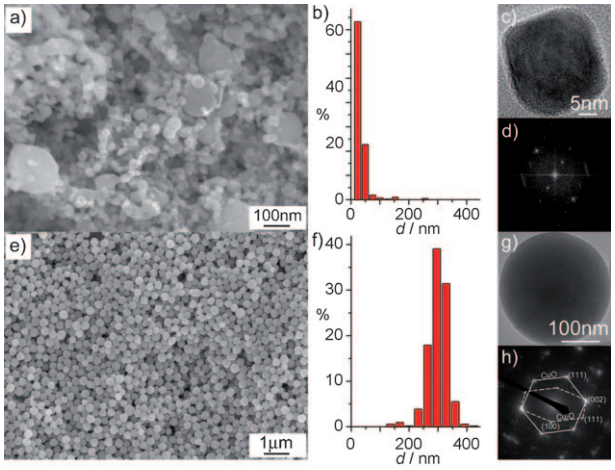

Figure 2. a–d) CuO raw nanoparticles: a) FESEM image, b) particle size distribution histogram (number proportion [%] for diameter *d*), c) TEM image, and d) SAED pattern. e–h) Submicrometer spheres obtained by pulsed laser irradiation of CuO nanoparticles in acetone (355 nm, 66 mJ pulse^{-1} cm^{-2}, 30 min): e) FESEM image, f) particle size distribution histogram, g) TEM image, and h) SAED pattern.

size of the raw nanoparticles is about 34 nm. The typical HRTEM image and corresponding fast Fourier transform pattern (Figure 2c,d) indicate that the CuO nanoparticles are single crystals. After pulsed laser irradiation (third harmonic, 30 min; Figure 2e), a large number of homogeneous spherical particles with an average size of 300 nm are produced. XRD analysis reveals that a phase change occurs after the laser irradiation (Supporting Information, Figure S1). A histogram by counting more than 400 particles is plotted in Figure 2f, indicating that the particle size distribution of the resulted submicrometer spheres is nearly mono-dispersed. A TEM image of a typical submicrometer sphere with a diameter of about 300 nm appears in Figure 2g, further confirming its spherical geometry, and the selected area electron diffraction pattern recorded from the edge of the sphere in Figure 2h indicates the single-crystalline nature.

It should be noted that size reduction is a well-known phenomenon in the process of pulsed laser irradiation of colloidal nanoparticles, and that many mechanisms have been proposed for the size reduction.[6] Interestingly, the present study clearly demonstrates that a size-increasing process occurs after the pulsed laser irradiation, and further experiments demonstrate this size increase can be controlled by input laser fluence. As seen in Figure 3a, when the laser

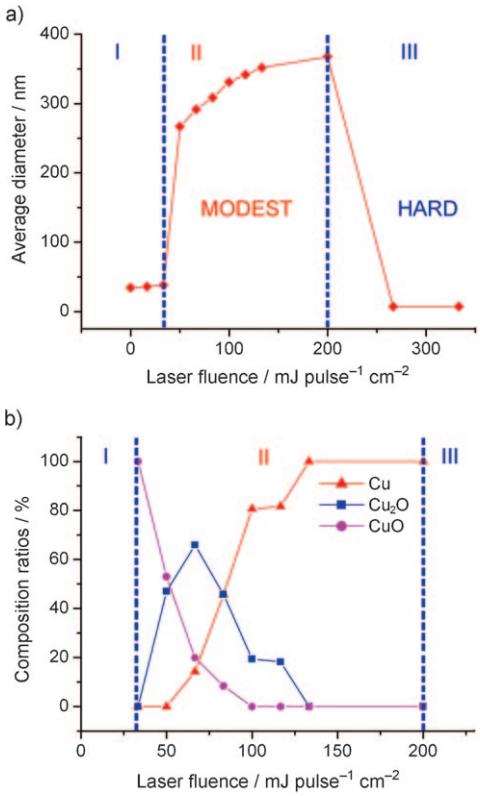

Figure 3. Laser-fluence-dependent size (a) and phase (b) changes in the pulsed laser irradiation (532 nm).

fluence is below 33 mJ pulse^{-1} cm^{-2}, the average particle sizes exhibit almost no change after the laser irradiation. Upon increasing the laser fluence from 50 to 200 mJ pulse^{-1} cm^{-2}, submicrometer spheres with an average diameter of 260 to 370 nm are obtained (Supporting Information, Figure S2). If the laser fluence is further increased to over 200 mJ pulse^{-1} cm^{-2}, the size of the obtained product dramatically decreases to below 10 nm (Supporting Information, Figure S3), indicating the evaporation of raw nanoparticles, a common phenomenon in hard laser irradiation.[6e] Because the size-increasing processes occur before the full evaporation of the raw nanoparticles (hard laser irradiation), we define these processes as modest laser irradiation.

Pulsed laser ablation in liquids is well-known for its extremely non-equilibrium conditions in which some unwanted metastable phases may appear.[7] However, owing to the specific intense reaction conditions, phase controllability becomes rather difficult when using this method. In the present study, an unfocused laser beam was utilized to irradiate the raw nanoparticles, thus providing relatively mild reaction conditions compared with the laser ablation technique. To investigate the feasibility of phase controllability under modest laser irradiation, the submicrometer

spheres obtained using different laser fluences were subjected to XRD measurements (Supporting Information, Figure S4). Figure 3b illustrates the phase-ratio evolution of the submicrometer spheres when the laser fluence is increased. When the laser fluence is below 33 mJ pulse^{-1} cm^{-2}, after the laser irradiation, the phases of the products is always CuO. When the laser fluence is increased to 50 mJ pulse^{-1} cm^{-2}, the CuO/Cu_2O phase appears, and further increasing the laser fluence leads to a gradual increase in metal copper phase and a decrease in CuO and Cu_2O. Finally, using a laser with a fluence exceeding 132 mJ pulse^{-1} cm^{-2} leads to the formation of pure metal copper phase. Thus the phase evolution may be related to the thermodynamic process. Furthermore, reductive gases resulting from the decomposition of acetone surrounding the melting spheres might also be responsible. This issue is currently being investigated further.

In the experiments conducted with a Nd:YAG laser, the heating–melting–evaporation mechanism is responsible for the size change.[6e] If a nanoparticle absorbs sufficient laser beam energy, it will melt or evaporate. To quantitatively define the specific fluence that results in the melting and evaporation of particles with given sizes, the Mie theory was used to calculate the absorption cross-section σ_{abs}^{λ}, for particles of different sizes d_p, and then to determine the energy absorbed by a particle irradiated by a single laser pulse [Equation (1)]:

$$Q_{abs}(\lambda,d_p) = J\sigma_{abs}^{\lambda}(d_p) \quad (1)$$

where J is the laser fluence. We assume that all of the energy absorbed by the particle will be spent on heating, melting, and evaporation [Eq. (2)] because the estimated possible heat losses are negligible compared to the energy absorbed by the particles from a laser pulse.[6c,e]

$$Q_{abs} = \rho_p(\pi d_p^3/6)\{C_p^s(T_m - T_0) + \Delta H_m + C_p^l(T_b - T_0) + \Delta H_b\} \quad (2)$$

Thus, the required laser fluence J^* for particles of different sizes that will heat a particle from T_0 (298.15 K) to the melting point T_m, to complete melting, to the boiling point T_b, and to full evaporation, can be determined. The physical and thermodynamic constants used in Equation (2), that is, the density ρ_p, the heat capacities C_p^s for solids and C_p^l for liquids, the melting heat ΔH_m, and the boiling heat ΔH_b, were adopted from JANAF.[8]

We now qualitatively discuss the size change according to the calculation result. Larger particles need higher energy to melt or evaporate owing to the large heat capacity of particles (Supporting Information, Figure S5), whereas smaller particles also require higher energy owing to the low optical cross-section of smaller particles in Cu-O system. When the laser fluence is much lower, nothing happens in the Cu-O system, and no particles melt. Particles with sizes of around 100–150 nm (see Figure 2a) start to melt with an increase in laser fluence, whereas small particles (below 50 nm) cannot melt. However, melted larger particles can take up smaller particles until all the smaller particles are consumed to exhibit homogenous size distribution (Supporting Information, Figure S6). A further increase of the laser fluence brings gradual particle size increase owing to merging of melted nearby particles. Within this fluence range, the obtained phase is gradually reduced upon laser fluence increase. The mechanism of these changes will be discussed in detail in future work. When the laser fluence increases beyond 200 mJ pulse^{-1} cm^{-2}, the resulting full evaporation of particles leads to a dramatic size decrease, as described in previous reports.[6]

Most importantly, modest laser irradiation for the synthesis of submicrometer spheres is suitable for many other kinds of semiconductor and metal nanoparticles, such as Ag, Au, Cu, Fe, Ni, Fe_2O_3, Fe_3O_4, Co_3O_4, NiO, TiO_2, WO_3, and ZnO, that exhibit optical absorption at 355 or 532 nm (for a Nd:YAG laser). Figure 4 shows some typical examples of the obtained submicrometer spheres by modest laser irradiation of corresponding commercial ZnO, WO_3, Cu, or Fe nanoparticles (Supporting Information, Figure S7). From the magnified SEM images in the insets, submicrometer spheres with smooth surfaces are not constructed by any nanostructured subunits.

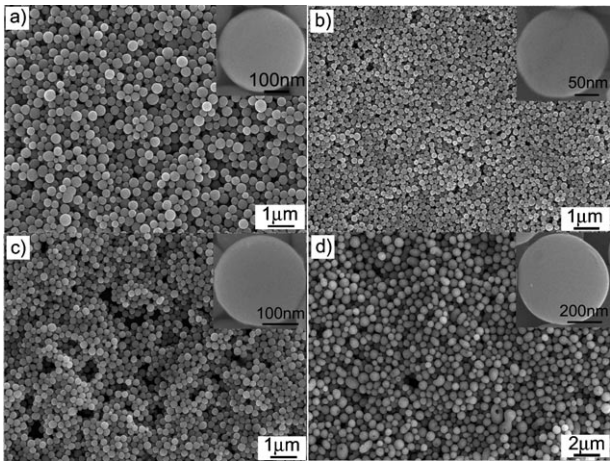

Figure 4. FESEM images of the submicrometer spheres obtained by the modest laser irradiation of commercial a) ZnO, b) WO_3, c) Cu, and d) Fe nanoparticles. Insets: magnified SEM images.

A typical difference between pulsed laser irradiation of colloidal nanoparticles and the laser ablation in liquid is that in pulsed laser irradiation the wavelength of the incident light is comparable to the size of target materials ($\lambda \approx d$), whereas in laser ablation, the incident light wavelength is much smaller than the target size ($\lambda \ll d$). One of the serious disadvantages of the technique of laser ablation in liquids is its ultralow productivity, usually amounting to several milligrams per hour.[9] However, in the present study, the transformation from nanoparticles to submicrometer spheres only took 30 seconds when we used a third-harmonic laser with a fluence of 132 mJ pulse^{-1} cm^{-2}. Therefore, the productivity of submicrometer spheres can reach about 100 mg h^{-1}, which is about two orders of magnitude greater than that using the technique of laser ablation in liquids. The greatly increased productivity and shortened reaction time are due to the reduction in size from bulk materials to nanoparticles and the resultant increased absorption efficiency of the laser beam.

In summary, we propose an innovative concept of selective pulsed heating, which is substantially different from conventional heating that usually relies on thermal conduction of black-body radiation to drive chemical reactions: 1) it is discontinuous, both temporally and spatially, and 2) it is easy to achieve an ultrahigh reaction temperature even in low-boiling-point solvents. By using this unique heating, we are the first to demonstrate the general synthesis of size-tailored semiconductor and metal submicrometer spheres, which are attracting significant research interest in many important fields. It is thus anticipated that this heating approach will tremendously advance the submicrometer-sphere-based technology. Encouragingly, compared with traditional technique of pulsed laser ablation in liquids, the PLICN technique presented in this paper provides mild reaction conditions, flexibility for size/phase control, and dramatically increased productivity, and thus may be adopted for industrial production. We believe that this facile laser irradiation approach represents a major step in the practical application of laser processing for materials synthesis.

Experimental Section

Materials synthesis: An Nd:YAG laser (Quanta Ray from Spectra-Physics; pulse width 10 ns, repetition rate 30 Hz) was used as the light source for pulsed laser irradiation. Typically, 0.8 mg of commercial CuO nanoparticles (Aldrich, < 50 nm, powder form) was first well-dispersed in 4 mL acetone by ultrasonic vibration. The mixture was then transferred to a sealed reaction cell and irradiated by an unfocused laser beam (66 mJ pulse^{-1} cm^{-2}, third harmonic) for 30 min.

Characterization: The phase, morphology and microstructure of the collected particles were measured and observed using a powder diffractometer (Rigaku; Ultima IV/PSK), a field emission scanning electron microscope (FESEM; Hitachi S4800), and a transmission electron microscope (TEM; JEOL 2010).

Received: May 17, 2010

Keywords: metals · nanoparticles · selective pulsed heating · semiconductors · submicrometer spheres

[1] a) Y. Wang, M. Ibisate, Z.-Y. Li, Y. Xia, *Adv. Mater.* **2006**, *18*, 471; b) J. Zhou, Y. Zhou, S. Buddhudu, S. L. Ng, Y. L. Lam, C. H. Kam, *Appl. Phys. Lett.* **2000**, *76*, 3513; c) M. Colilla, M. Manzano, I. Izquierdo-Barba, M. Vallet-Regí, C. Boissiére, C. Sanchez, *Chem. Mater.* **2010**, *22*, 1821; d) W. Zhao, H. Chen, Y. Li, L. Li, M. Lang, J. Shi, *Adv. Funct. Mater.* **2008**, *18*, 2780; e) J. E. Lee, N. Lee, H. Kim, J. Kim, S. H. Choi, J. H. Kim, T. Kim, I. C. Song, S. P. Park, W. K. Moon, T. Hyeon, *J. Am. Chem. Soc.* **2010**, *132*, 552; f) C. C. Li, X. M. Yin, T. H. Wang, H. C. Zeng, *Chem. Mater.* **2009**, *21*, 4984; g) J. Zhang, J. Liu, Q. Peng, X. Wang, Y. Li, *Chem. Mater.* **2006**, *18*, 867; h) X. Hu, J. Gong, L. Zhang, J. C. Yu, *Adv. Mater.* **2008**, *20*, 4845; i) Y. Li, T. Sasaki, Y. Shimizu, N. Koshizaki, *J. Am. Chem. Soc.* **2008**, *130*, 14755; j) C. Guo, M. Ge, L. Liu, G. Gao, Y. Feng, Y. Wang, *Environ. Sci. Technol.* **2010**, *44*, 419; k) Q. Zhang, C. Dandeneau, S. Candelaria, D. Liu, B. B. Garcia, X. Zhou, Y. H. Jeong, G. Cao, *Chem. Mater.* **2010**, *22*, 2427; l) J. H. Park, S. Y. Jung, R. Kim, N. G. Park, J. Kim, S. S. Lee, *J. Power Sources* **2009**, *194*, 574; m) Y. Kondo, H. Yoshikawa, K. Awaga, M. Murayama, T. Mori, K. Sunada, S. Bandow, S. Iijima, *Langmuir* **2008**, *24*, 547.

[2] a) A. E. Nel, L. Mädler, D. Velegol, T. Xia, E. M. V. Hoek, P. Somasundaran, F. Klaessig, V. Castranova, M. Thompson, *Nat. Mater.* **2009**, *8*, 543; b) G. Bhabra, A. Sood, B. Fisher, L. Cartwright, M. Saunders, W. H. Evans, A. Surprenant, G. Lopez-Castejon, S. Mann, S. A. Davis, L. A. Hails, E. Ingham, P. Verkade, J. Lane, K. Heesom, R. Newson, C. P. Case, *Nat. Nanotechnol.* **2009**, *4*, 876.

[3] a) S. H. Im, U. Y. Jeong, Y. Xia, *Nat. Mater.* **2005**, *4*, 671; b) W. Stöber, A. Fink, E. Bohn, *J. Colloid Interface Sci.* **1968**, *26*, 62.

[4] a) X. Jiang, T. Herricks, Y. Xia, *Adv. Mater.* **2003**, *15*, 1205; b) Y. Wang, Y. Xia, *Nano Lett.* **2004**, *4*, 2047; c) Y. Wang, L. Cai, Y. Xia, *Adv. Mater.* **2005**, *17*, 473; d) U. Jeong, Y. Wang, M. Ibisate, Y. Xia, *Adv. Funct. Mater.* **2005**, *15*, 1907.

[5] a) F. Caruso, R. A. Caruso, H. Möhwald, *Science* **1998**, *282*, 1111; b) D. Chen, L. Cao, F. Huang, P. Imperia, Y. B. Cheng, R. A. Caruso, *J. Am. Chem. Soc.* **2010**, *132*, 4438; c) Y. Wang, G. Wang, H. Wang, C. Liang, W. Cai, L. Zhang, *Chem. Eur. J.* **2010**, *16*, 3497; d) W. W. Wang, Y. J. Zhu, L. X. Yang, *Adv. Funct. Mater.* **2007**, *17*, 59.

[6] a) A. Pyatenko, M. Yamaguchi, M. Suzuki, *J. Phys. Chem. C* **2007**, *111*, 7910; b) S. Link, M. El-Sayed, *J. Phys. Chem. B* **1999**, *103*, 4212; c) A. Takami, H. Kurita, S. Koda, *J. Phys. Chem. B* **1999**, *103*, 1226; d) P. V. Kamat, M. Flumiani, G. V. Hartland, *J. Phys. Chem. B* **1998**, *102*, 3123; e) A. Pyatenko, M. Yamaguchi, M. Suzuki, *J. Phys. Chem. C* **2009**, *113*, 9078.

[7] a) P. Liu, Y. L. Cao, C. X. Wang, X. Y. Chen, G. W. Yang, *Nano Lett.* **2008**, *8*, 2570; b) P. Liu, Y. L. Cao, X. Y. Chen, G. W. Yang, *Cryst. Growth Des.* **2009**, *9*, 1390; c) Y. Ishikawa, Y. Shimizu, T. Sasaki, N. Koshizaki, *Appl. Phys. Lett.* **2007**, *91*, 161110; d) H. B. Zeng, W. P. Cai, J. L. Hu, G. T. Duan, P. S. Liu, Y. Li, *Appl. Phys. Lett.* **2006**, *88*, 171910.

[8] JANAF Thermochemical Tables **1974** supplement.

[9] a) G. W. Yang, *Prog. Mater. Sci.* **2007**, *52*, 648; b) W. T. Nichols, T. Sasaki, N. Koshizaki, *J. Appl. Phys.* **2006**, *100*, 114912.

